Mutual nonlinear prediction as a tool to evaluate coupling strength and directionality in bivariate time series: Comparison among different strategies based on *k* nearest neighbors

Luca Faes,[1,*] Alberto Porta,[2] and Giandomenico Nollo[1]
[1]*Department of Physics, University of Trento, Trento, Italy*
[2]*Department of Technologies for Health, Galeazzi Orthopaedic Institute, University of Milan, Milan, Italy*
(Received 25 February 2008; published 1 August 2008)

We compare the different existing strategies of mutual nonlinear prediction regarding their ability to assess the coupling strength and directionality of the interactions in bivariate time series. Under the common framework of *k*-nearest neighbor local linear prediction, we test three approaches based on cross prediction, mixed prediction, and predictability improvement. The measures of interdependence provided by these approaches are first evaluated on short realizations of bivariate time series generated by coupled Henon models, investigating also the effects of noise. The usefulness of the three mutual nonlinear prediction schemes is then assessed in a common physiological application during known conditions of interaction—i.e., the analysis of the interdependence between heart rate and arterial pressure variability in healthy humans during supine resting and passive head-up tilting. Based on both simulation results and physiological interpretability of cardiovascular results, we conclude that cross prediction is valuable to quantify the coupling strength and predictability improvement to elicit directionality of the interactions in short and noisy bivariate time series.

DOI: 10.1103/PhysRevE.78.026201 PACS number(s): 05.45.Tp, 05.45.Xt, 87.19.Hh

I. INTRODUCTION

In past decades, the detection and characterization of the interdependence among dynamical systems has gained increasing importance and has found relevant applications in many physical fields. As an example, the study of the coupling between simultaneously collected physiological signals has been widely used to investigate interactions within neurophysiological [1] and cardiovascular [2,3] systems. Recently a large variety of methods—e.g., based on concepts from information theory [4], phase synchronization [5], and state space correspondence [6–8]—have been proposed to detect interdependences in nonlinear dynamical systems. Among them, approaches based on mutual nonlinear prediction [9–15] have shown their usefulness in practical applications thanks to their suitability to deal with real physiological signals, which are commonly noisy and are stationary only for short data sequences.

The study of the interdependence between two dynamical systems **X** and **Y** in terms of mutual nonlinear prediction is based on the rationale that in the presence of coupling the time series x and y measured from the systems are mutually predictable, where mutual predictability is defined as the ability to predict one of the two series based on knowledge of state vectors including points of the other series. Within this framework, three approaches which directly exploit mutual nonlinear prediction to evaluate the coupling between dynamical systems have been proposed in the past: cross prediction—i.e., the prediction of a time series starting from the dynamics of the other series in its embedded state space—was introduced to detect dynamical interdependence and generalized synchronization in chaotic systems [9]; mixed prediction—i.e., the prediction of a time series starting from mixed states consisting of samples taken from both the considered series—was proposed to detect weak couplings below the onset of generalized synchronization [11]; predictability improvement—i.e., the increase in the predictability degree brought by mixed prediction with respect to the self-prediction of a single time series—was introduced as an asymmetrical measure of nonlinear interdependence between two series [12]. Although they have not been directly compared yet, these approaches are supposed to show different capabilities to detect the coupling between interacting systems, depending on the nature (e.g., unidirectional or bidirectional) and on the strength of such coupling.

Another important issue in coupling analysis is the determination of directionality of the interactions. Although there has been no universally accepted definition of causality [16], it is common belief that the notion of causality between two events describes to what extent one event is caused by the other. With implicit reference to this general concept, a large number of methods have been proposed to infer causality from the asymmetry of various interdependence measures [3,4,7,8,17–19]. These methods identified the existence of a driver-response relationship between two time series x and y when a stronger dependence was found in one of the two causal directions (i.e., from x to y and from y to x) according to the proposed asymmetrical coupling measure. This approach can be followed also by the three methods performing mutual nonlinear prediction presented above [9–12]. Indeed, since the corresponding coupling measures are asymmetrical, the prevailing coupling direction might be inferred by looking at the difference between the measures obtained after exchanging the roles of the series x and y during mutual nonlinear prediction. However, it has been shown that interpretation of causality based on the asymmetry of coupling measures can be contradictory. For instance, the authors of [9,10] made opposite claims about the coupling direction using the same cross-prediction approach on simulated unidi-

*Corresponding author: Lab. Biosegnali, Dipartimento di Fisica, Università di Trento via Sommarive 14, 38050 Povo, Trento, Italy. FAX: +39 0461 881696. faes@science.unitn.it.

rectionally coupled systems. In fact, previous studies using observables different from nonlinear predictability [17,20] demonstrated that inferring directionality from the asymmetry of coupling measures is often difficult, as it may depend on differences between the dynamical properties of the two investigated systems and on the strength of their coupling.

A specific definition of causality between two time series was that proposed by Wiener [21] and later formalized by Granger [22]. According to this definition, the series x is called causal to the series y if we can predict y better using the past information from x than by using the information without it. The concept of Granger causality, originally proposed in the context of linear regression models of stochastic processes [22], has been recently extended to nonlinear systems [13,14]. As can be deduced from the definition, this concept, either approached within a linear or a nonlinear framework, is intimately related to the mutual prediction of bivariate time series. Particularly, measures quantifying how much the prediction of one series is improved by incorporating points of the other series in the prediction scheme [12–14] make direct reference to Granger's approach to the evaluation of causality.

In the present study we compare the different existing conceptual approaches proposed to perform mutual nonlinear prediction of bivariate time series in relation to their ability to quantify coupling strength and directionality. To this end, measures of nonlinear interdependence based on cross prediction, mixed prediction, and predictability improvement are evaluated on simple well-known numerical simulations, as well as on real data taken from the cardiovascular system. In order to facilitate the comparison, a common methodological framework—i.e., nonlinear prediction based on the k-nearest-neighbor local linear approximation [23,24]—as well as a common observable—i.e., the squared correlation between original and predicted data [25]—are used to apply the three prediction schemes. To assess the applicability of the considered nonlinear interdependence measures to real physiological conditions, simulations are performed on short bivariate time series, and the effects of noise are also taken into account. The subsequent application to heart rate and arterial pressure series measured from healthy humans is aimed at testing the physiological interpretability of the measures.

II. METHODS

A. Local approximation approaches to perform mutual nonlinear prediction

Let the two time series $x=\{x_i, i=1,\ldots,N\}$ and $y=\{y_i, i=1,\ldots,N\}$ be observable variables simultaneously measured from two potentially coupled dynamical (sub)systems **X** and **Y**, respectively. Since time series from different systems generally do not span the same range of values, x and y are first normalized to zero mean and unit variance. Using the time delay embedding technique [26], the two series are then embedded in a mixed state space by constructing state vectors including m samples of x and n samples of y, $\mathbf{z}_i=[x_i,x_{i-l},\ldots,x_{i-(m-1)l},y_i,y_{i-l},\ldots,y_{i-(n-1)l}]$, where l is the time lag. Mutual nonlinear prediction of the two series is performed by assuming functional nonlinear relationships between the current state $\mathbf{z}_i$ and the future values x_{i+l} and y_{i+l}:

$$x_{i+l}=f(\mathbf{z}_i), \quad y_{i+l}=g(\mathbf{z}_i), \tag{1}$$

where f and g are estimated by means of a local linear approximation approach—i.e., by fitting an hyperplane to the k nearest neighbors of $\mathbf{z}_i$ in the mixed state space of **X** and **Y** [23]. Specifically, let $s_{i,j}$, $j=1,\ldots,k$, denote the time indices of the k Euclidean nearest neighbors of the current state $\mathbf{z}_i$. The neighbors $\mathbf{z}_{s_{i,j}}$, $j=1,\ldots,k$, are kept separated from the current state $\mathbf{z}_i$ by using a Theiler window of width $(m+n)l$ samples [27] in order to prevent temporal correlations between the reference vector and its selected neighbors, as well as to perform an out-of-sample prediction [15]. Two systems of k linear equations, each involving the k nearest neighbors, are then defined as

$$x_{s_{i,j}+l}=\boldsymbol{\alpha}\cdot\mathbf{z}_{s_{i,j}}, \quad y_{s_{i,j}+l}=\boldsymbol{\beta}\cdot\mathbf{z}_{s_{i,j}}, \quad j=1,\ldots,k. \tag{2}$$

The systems are then solved by least-squares optimization to yield the estimates $\hat{\boldsymbol{\alpha}}$ and $\hat{\boldsymbol{\beta}}$ of the vector coefficients $\boldsymbol{\alpha}$ and $\boldsymbol{\beta}$, which are finally used to predict the future values of the two series

$$\hat{x}_{i+l}=\hat{\boldsymbol{\alpha}}\cdot\mathbf{z}_i, \quad \hat{y}_{i+l}=\hat{\boldsymbol{\beta}}\cdot\mathbf{z}_i. \tag{3}$$

After predicting Nr values, the squared correlation between the predicted and the original future values of the series x,

$$\rho_x^2=\left(\sum_{i=1}^{Nr}x_{i+l}\hat{x}_{i+l}\right)^2\Bigg/\sum_{i=1}^{Nr}x_{i+l}^2\sum_{i=1}^{Nr}\hat{x}_{i+l}^2, \tag{4}$$

is taken as a measure of the predictability of the series [25]. The same holds for the series y, for which the squared correlation is ρ_y^2. These two predictability measures are bounded between 0 and 1, with 0 indicating full unpredictability and 1 full predictability of the investigated dynamics.

With fixed embedding lag l and number of neighbors, k, the degrees of predictability of the two series are a function of the embedding dimensions m and n—that is, $\rho_x^2=\rho_x^2(m,n)$ and $\rho_y^2=\rho_y^2(m,n)$. In the following we will indicate with self-embedding dimension the number of samples of a series used to predict the future of the same series (i.e., m for the prediction of x and n for the prediction of y) and with cross-embedding dimension the number of samples of a series used to predict the future of the other series (i.e., n for the prediction of x and m for the prediction of y). Setting to zero the cross-embedding dimension corresponds to perform *self-prediction*, setting to zero the self-embedding dimension corresponds to perform *cross prediction*, and letting both $m>0$ and $n>0$ corresponds to perform *mixed prediction* of a given time series. With these prediction schemes, three different predictability functions—respectively, quantifying the self-predictability, cross predictability, and mixed predictability of the two time series—can be defined using the observable of Eq. (4):

$$P_{Sx}(m)=\rho_x^2(m,0), \quad P_{Sy}(n)=\rho_y^2(0,n),$$

$$P_{Cx}(n)=\rho_x^2(0,n), \quad P_{Cy}(m)=\rho_y^2(m,0),$$

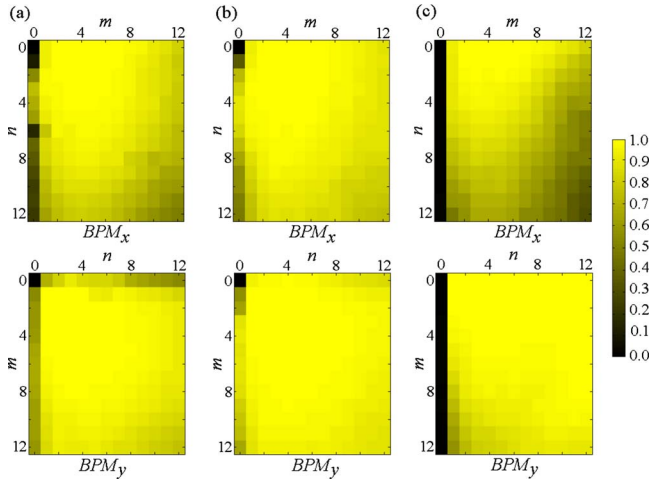

FIG. 1. (Color online) Representative examples of bivariate predictability maps (BPMs) obtained for unidirectionally coupled nonidentical Henon maps [(a) Eq. (10) with $c=0.6$], bidirectionally coupled nonidentical Henon maps [(b) Eq. (11) with $c_1=0.2$ and $c_2=0.05$], and uncoupled nonidentical Henon maps [(c) Eq. (10) with $c=0$]. The maps depict color-coded values of the squared correlation between original series and series predicted from mixed states with m samples of x and n samples of y.

$$P_{Mx}(m,n)=\rho_x^2(m,n), \quad P_{My}(m,n)=\rho_y^2(m,n), \quad m,n \geqslant 1. \tag{5}$$

A convenient way to represent together these predictability functions is to realize bivariate predictability maps (BPMs), which are diagrams reporting the color-coded values of the observable defined in Eq. (4) as a function of the self- and cross-embedding dimensions ranging from 0 to a given maximum (12 in this work). A representative example is reported in Fig. 1. In each BPM, the self-embedding dimension varies across the columns and the cross-embedding dimension across the rows of the map. In this way, the predictability yielded by self-prediction (i.e., the function P_S) is represented by the first row of the BPM and the predictability yielded by cross prediction (i.e., the function P_C) is represented by the first column of the BPM, while the remaining part of the BPM corresponds to mixed prediction (i.e., to the function P_M).

In the following sections, mutual nonlinear prediction will be performed in both numerical simulations and real data applications. For each pair of bivariate time series, the two maps indicating the predictability of x and y as a function of the embedding dimensions (BPMx and BPMy) are evaluated, and representative measures of nonlinear interdependence along a predefined temporal direction (i.e., from y to x in the case of BPMx and the reverse in the case of BPMy) are then provided according to approaches previously proposed in the literature.

(i) The cross-prediction approach quantifies interdependence as the predictability of one of the two series estimated using state space vectors of the other series [9]:

$$S_{1x}=\max_n\{P_{Cx}(n)\}, \quad S_{1y}=\max_m\{P_{Cy}(m)\}. \tag{6}$$

(ii) The mixed-prediction approach quantifies interdependence as the predictability of a series using state vectors that contain samples of both series [11]:

$$S_{2x}=\max_{m,n}\{P_{Mx}(m,n)\}, \quad S_{2y}=\max_{m,n}\{P_{My}(m,n)\}. \tag{7}$$

(iii) The predictability-improvement approach quantifies interdependence as the increase in predictability yielded by mixed prediction compared to self-prediction [12]:

$$S_{3x}=\max_{m,n}\{P_{Mx}(m,n)\}-\max_m\{P_{Sx}(m)\},$$
$$S_{3y}=\max_{m,n}\{P_{My}(m,n)\}-\max_n\{P_{Sy}(n)\}. \tag{8}$$

In addition to the directional measures of Eqs. (6)–(8), we define nondirectional interdependence measures by taking the maximum of the two directional coupling values for the considered bivariate time series—i.e., $S_1=\max\{S_{1x},S_{1y}\}$, $S_2=\max\{S_{2x},S_{2y}\}$, and $S_3=\max\{S_{3x},S_{3y}\}$—defined as a measure of synchronization in [28]. While the nondirectional measures are used to quantify the coupling strength, asymmetries between the two directional measures are exploited to infer driver-response relationships (i.e., the coupling direction).

The indices S_1, S_2, and S_3 refer, respectively, to cross prediction, mixed prediction, and predictability improvement. Since calculation of the index S_3 as originally proposed by [12] directly involves self-prediction [see Eq. (8)], the predictability of the single time series may affect the corresponding coupling measure. To circumvent this problem, some authors have proposed to normalize the predictability improvement to the self-unpredictability of the time series under investigation [14]. According to this modification, we also compute the normalized predictability improvement as

$$S_{3Nx}=\frac{S_{3x}}{1-\max_m\{P_{Sx}(m)\}}, \quad S_{3Ny}=\frac{S_{3y}}{1-\max_n\{P_{Sy}(n)\}}, \tag{9}$$

and calculate the corresponding nondirectional measure of coupling as $S_{3N}=\max\{S_{3Nx},S_{3Ny}\}$ [28].

B. Surrogate data approach

We used the method of surrogate data [29] to test the hypothesis that the two considered time series are uncoupled. In this work, we used time-shifted signals as realizations of surrogate time series and compared predictability at short lags (l samples) with predictability at randomly selected long lags ($>20l$ samples). Time-shifted bivariate surrogate data were generated by leaving unchanged the time series that had to be predicted, while shifting over time the other time series and wrapping the extra values around the beginning of the series. One hundred shift lags were chosen randomly with the restriction that shifts be larger than $20l$ samples. The threshold for significance of the coupling was set at the upper 95th percentile of the distribution of the coupling index calculated for the surrogate pairs. With respect to traditional surrogates based on phase randomization of the Fourier transform [30], time-shifted surrogates preserve the whole

statistical structure of both original time series, blunting the short lag correlations in the original data. Hence, they are indicated to test the significance of the asymmetry of directional measures of coupling [8,31]. The use of surrogates maintaining the intrinsic dimensionality of the original series allows us indeed to reject the hypothesis of differences in complexity as the prime reason explaining any reported coupling asymmetry. This aspect is particularly relevant when dealing with nonlinear interdependence measures that have been shown to be potentially affected by the different dynamical properties of the two series [8,31,32].

The bivariate surrogate data here generated provide a threshold for significance for cross prediction and mixed prediction, and obviously not for self-prediction. As a consequence, the significance of S_2 and S_3 is always the same when evaluated by these bivariate surrogates. Nevertheless, in this study we considered as not significant even the coupling corresponding to $S_3<0$ (and thus $S_{3N}<0$), as in the presence of stationary time series negative predictability improvements cannot be interpreted in ways other than a signature of independence.

III. NUMERICAL EXAMPLES

In this section we report the application of mutual nonlinear prediction to known simulated signals, performed to test its ability in evaluating coupling and causality during different conditions of interaction. In order to discuss the properties of each predictor in terms of already existing results, we studied the Henon system, which was taken into consideration by several previous reports dealing with mutual nonlinear prediction of time series [9,11,12,15]. Moreover, short realizations of the dynamics ($N=500$ points) were considered to match requirements of the practical application on real physiological data, which are often limited to few hundred points to fulfill stationarity constraints. These choices leave to future applications the evaluation of approaches based on mutual nonlinear prediction on high-dimensional continuous systems such as those including time delays, as well as the study of the effects of nonstationarities over the assessment of coupling strength and directionality.

We considered different types of interaction (uncoupling, unidirectional coupling, bidirectional coupling), as well as different coupling strengths for the coupled systems. Furthermore, the analysis was repeated for Henon systems with identical and nonidentical parameters, and the robustness of the various measures against noise corruption of the dynamics was also studied. From each pair of Henon systems, time series lasting 500 points were taken after discarding the systems' initial transient responses. The initial conditions were always set at identical values for the two systems. The embedding time lag was set to $l=1$, and $k=30$ neighbors were used for local linear prediction. No significant changes were observed for other values of k.

A. Unidirectionally coupled systems

As a first example we considered two unidirectionally coupled Henon maps [9], defined by the equations

$$x_{i+1} = 1.4 - x_i^2 + 0.3u_i, \quad u_{i+1} = x_i, \tag{10a}$$

$$y_{i+1} = 1.4 - [cx_i + (1-c)y_i]y_i + bv_i, \quad v_{i+1} = y_i, \tag{10b}$$

where the constant b was set to 0.3 to have identical systems and to 0.1 to have nonidentical systems. The constant c modulates the strength of the coupling from x to y and was varied from 0.1 to 1, step 0.1. The case $c=0$ corresponds to uncoupled dynamics and will be discussed separately in Sec. III C. An example of BPMs obtained for unidirectionally coupled maps with $b=0.1$ and $c=0.6$ is reported in Fig. 1(a). The values of the coupling indices in this example are $S_{1x}=0.739$, $S_{1y}=0.662$; $S_{2x}=0.999$, $S_{2y}=0.998$; $S_{3x}=-0.0004$, $S_{3y}=0.082$; $S_{3Nx}=-2.173$, and $S_{3Ny}=0.982$.

The directional measures of coupling [Eqs. (6)–(9)] calculated as a function of c for identical systems and nonidentical systems are reported in Figs. 2 and 3, respectively. The corresponding nondirectional coupling measures can be easily derived by taking the higher of the two directional values for a given value of c. While the index S_1 shows a clear tendency to increase with the coupling strength [Figs. 2(a), 2(e), 3(a), and 3(e)], all other measures seem not able to reflect the imposed degree of unidirectional coupling. These results suggest that the approach based on cross prediction is capable of evaluating the strength of the coupling in bivariate time series. On the contrary, the responsiveness to the coupling strength of interdependence measures yielded by mixed-prediction and predictability-improvement approaches may be obscured by the quote of self-predictability due to the inclusion of past points of the investigated series into the prediction scheme.

In the case of identical systems, both S_{1x} and S_{1y} are always significantly larger than the surrogate threshold for all values of c [Fig. 2(a)]. Moreover, the maximal cross predictability is generally higher in the direction from y to x than vice versa ($S_{1x} \geqslant S_{1y}$). Although a bit counterintuitive with respect to the imposed unidirectional interaction from x to y, this result is in agreement with those of Ref. [9], also found in Ref. [17] using measures of nonlinear interdependence based on observables different from mutual prediction. S_{1x} and S_{1y} take on exactly the same values for $c=0.5$, when generalized synchronization sets in, and for $c>0.7$, when the systems fall in a region of identical synchronization [17]. This is not surprising, since during synchronization regimes the mapping of closeness in the state space is reciprocal, so that mutual prediction returns identical predictability degrees in the two directions. Analogous results were observed with S_2 [Fig. 2(b)], even though the result is less evident from the index values due to the high degree of self-predictability captured by mixed prediction that masks the information about coupling. On the contrary, S_3 and S_{3N} exhibit a different behavior [Figs. 2(c) and 2(d)]. S_{3x} and S_{3Nx} are never significant, due to the negative predictability improvement always measured for the series x. When synchronization is not occurring ($c \leqslant 0.7$, $c \neq 0.5$), S_{3y} and S_{3Ny} are always statistically significant, thus detecting the unidirectional coupling and the presence of Granger causality from x to y. When synchronization sets in, both S_{3x} and S_{3y}, as well as S_{3Nx} and S_{3Ny}, are not significant, indicating that the inclu-

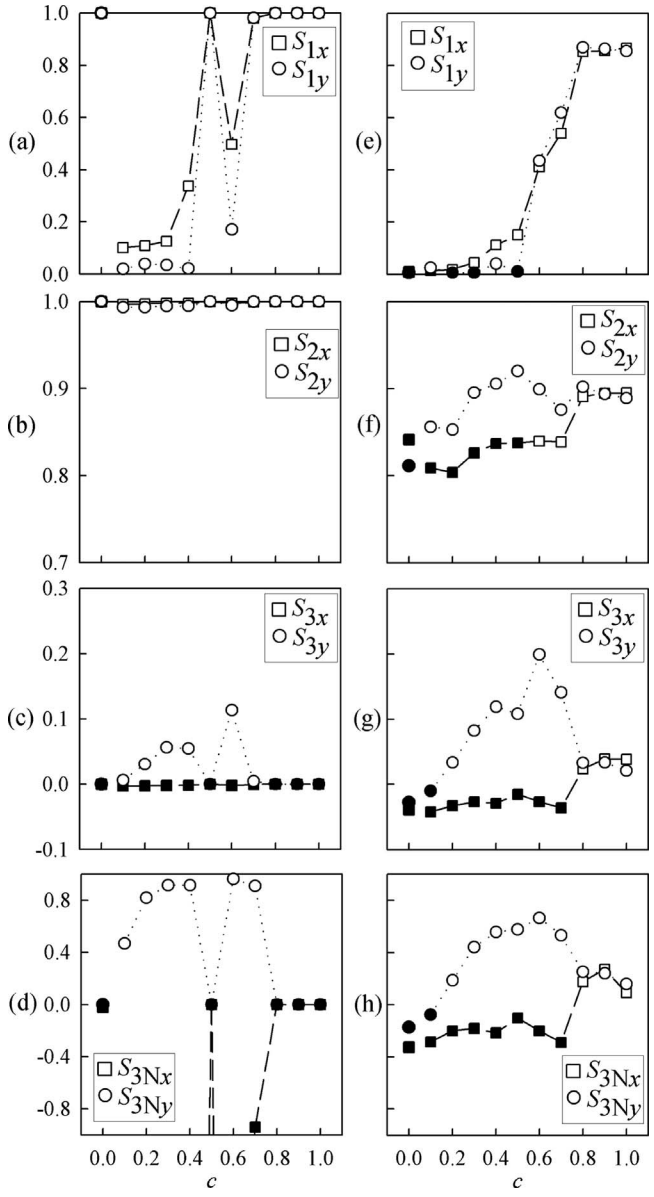

FIG. 2. Measures of synchronization obtained by cross prediction (S_1), mixed prediction (S_2), and predictability improvement (S_3 and S_{3N}), plotted as a function of the coupling strength c imposed in unidirectionally coupled identical Henon maps [Eq. (10), $b=0.3$]. Results in panels (a), (b), (c), and (d) are for the noise-free realizations and in panels (e), (f), (g), and (h) for the realizations with inclusion of system and measurement noise. Interactions measured in the direction from x to y and from y to x are represented by circles and squares, respectively. Solid symbols indicate synchronization values not statistically different from zero according to surrogate data analysis.

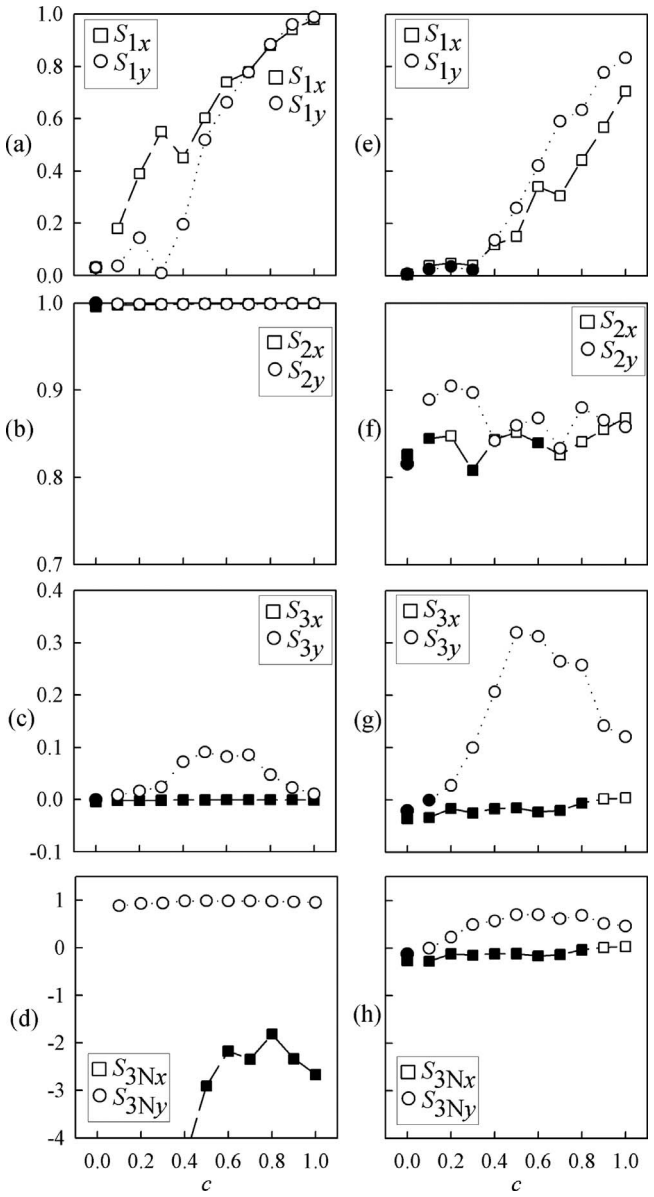

FIG. 3. Same as Fig. 2 for unidirectionally coupled nonidentical Henon maps [Eq. (10), $b=0.1$].

sion of the second series does not provide additional information to the prediction of the first one. This result is expected, since for fully synchronized systems driver and response are indistinguishable from each other [12], so that the predictability improvement cannot reflect the actual coupling strength and Granger causality cannot be assessed.

The above discussion holds similarly for nonidentical systems [Figs. 3(a)–3(d)], with the exception that here full synchronization between the systems is not achievable and thus asymmetry in the interdependence measures is expected for all coupling strengths. In fact, S_1, S_2, S_3, and S_{3N} are never the same in the two directions as happened during generalized or identical synchronization for identical systems. Again, the directional coupling evaluated by cross prediction is larger from y to x than in the opposite direction [$S_{1x} > S_{1y}$, Fig. 3(a)], but this information is lost for high coupling strengths ($c>0.7$). Mixed prediction is no more able to elicit the direction of coupling, as we found $S_{2x}>S_{2y}$ or $S_{2y}>S_{2x}$ depending on the coupling degree. Predictability improvement and normalized predictability improvement are able to elicit causality from x to y, as we observe $S_{3y}>S_{3x}$ and $S_{3Ny}>S_{3Nx}$ for all values of c [Figs. 3(c) and 3(d)]. This suggests that, even if the driver has higher dimension than the driven system, measures based on the predictability improvement are able to set the correct direction of interaction

(from x to y in this case). On the contrary, measures based on cross prediction [9,10] or closeness in the state space [17,31] tend to favor the system with more excited degrees of freedom (the system **X** in this case) [6,7,17]. As happened for identical systems, S_1 and S_2 are always larger than their corresponding threshold for significance in both directions and for all values of c, while S_3 and S_{3N} are always significant from x to y, thus detecting Granger causality, and never significant from y to x, thus detecting the unidirectional nature of the coupling.

We also studied how the three measures changed with the inclusion of both system noise (with standard deviation =0.005) and measurement noise (with standard deviation =0.2). Results for identical and nonidentical systems are shown in Figs. 2(e)–2(h) and in Figs. 3(e)–3(h), respectively. In general, it is of course expected that all predictions become worse in presence of noise. In fact, S_1 and S_2 decrease as a consequence of the lower correlation between original and predicted data yielded by cross and mixed predictions. For the same reason, these two indices may become nonsignificant in the presence of low coupling strengths [e.g., see Figs. 2(e), 2(f), 3(e), and 3(f)]. As to S_3, it shows a general increase with respect to the noise-free condition [Figs. 2(g) and 3(g)]. This effect is explained by considering that noise inclusion worsens also the self-prediction of the time series, which was very good (i.e., associated with very high ρ^2 values) for the clean maps. Due to index normalization, the increase of the predictability improvement in the presence of noise is not observed for S_{3N}. Both predictability improvement indices are still able to detect the directional relationship [$S_{3y} \geqslant S_{3x}$, $S_{3Ny} \geqslant S_{3Nx}$, Figs. 2(g), 2(h), 3(g), and 3(h)], with the only drawback that noise can make the index insignificant in case of low coupling (e.g., with $c=0.1$) or significant in both directions in the case of high coupling (e.g., with $c>0.8$). On the contrary, the interpretation of the directional information given by S_1 and S_2 is controversial even during noise corruption. In fact, the asymmetry of S_1 and S_2 was reversed after noise addition in some cases [e.g., we observe $S_{2x}>S_{2y}$ in Fig. 2(b) and $S_{2y}>S_{2x}$ in Fig. 2(f) or $S_{1x}>S_{1y}$ in Fig. 3(a) and $S_{1y}>S_{1x}$ in Fig. 3(e)], or resulted dependent on the coupling strength in some other cases [e.g., see Figs. 2(e) and 3(f)].

It is worth noting that the normalization procedure applied to the predictability improvement affected the absolute value, but did not alter the behavior of the index at varying the imposed degree of coupling. Indeed, in all conditions the trends of S_{3Nx} and S_{N3y} [Figs. 2(d), 2(h), 3(d), and 3(h)] mimic those of S_{3x} and S_{3y} [Figs. 2(c), 2(g), 3(c), and 3(g)]. This result is explained by the fact that, in the simulations considered, the self-predictability of the series was not substantially modified at varying the coupling strength.

B. Bidirectionally coupled systems

In the second example, we study two bidirectionally coupled Henon maps [11], with the equations

$$x_i = 1.4 - x_{i-1}^2 + 0.3x_{i-2} + c_2(x_{i-1}^2 - y_{i-1}^2),$$

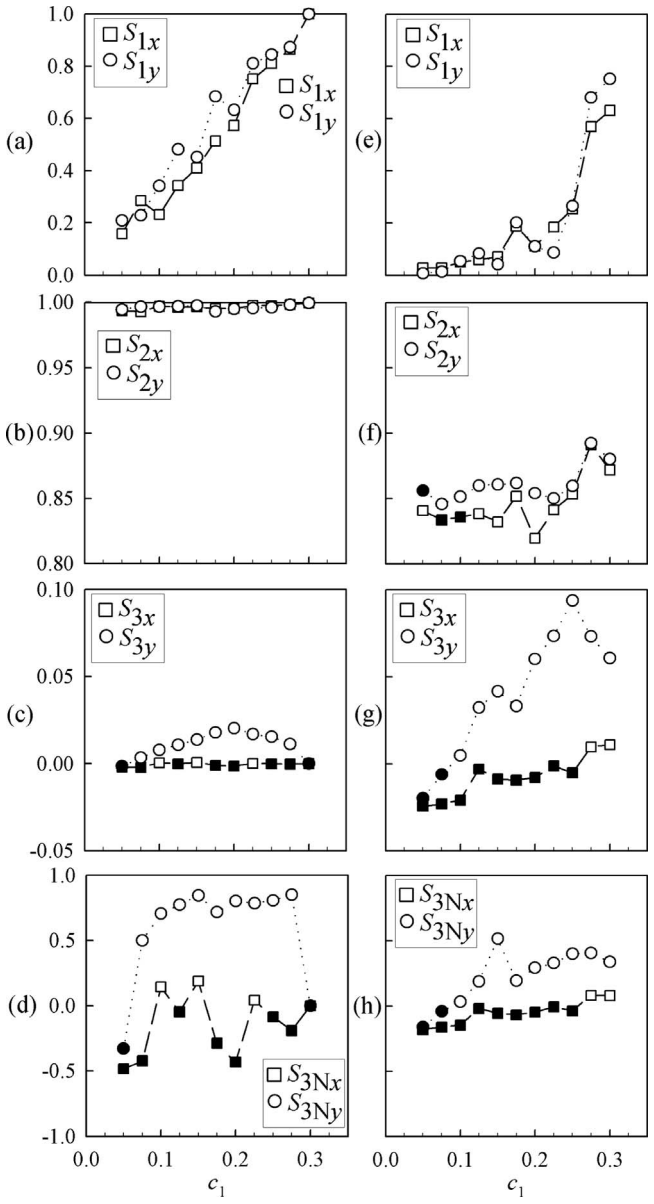

FIG. 4. Same as Fig. 2 for bidirectionally coupled identical Henon maps [Eq. (11), $b=0.3$]. Plots represent synchronization values as a function of the coupling strength from x to y (c_1), with coupling strength from y to x given by $c_2=0.05$.

$$y_i = 1.4 - y_{i-1}^2 + by_{i-2} + c_1(y_{i-1}^2 - x_{i-1}^2), \qquad (11)$$

where the constants c_1 and c_2 determine the strength of coupling in the directions from x to y and from y to x, respectively. Again, b was set to 0.3 to have identical systems and to 0.1 to have nonidentical systems. In the simulations, c_1 was varied from 0.05 to 0.3, while keeping constant c_2 =0.05. An example of the BPMs obtained setting $c_1=0.2$ and $c_2=0.05$ (with $b=0.1$) is shown in Fig. 1(b). The values of the coupling indices in this example are $S_{1x}=0.897$, S_{1y} =0.911; $S_{2x}=0.9995$, $S_{2y}=0.9990$; $S_{3x}=0.0005$, $S_{3y}=0.0118$; and $S_{3Nx}=0.512$, $S_{3Ny}=0.923$. The complete results are reported in Figs. 4 and 5. For $c_1=c_2=0.05$ we have balanced bidirectional coupling, while in all other cases there is bidi-

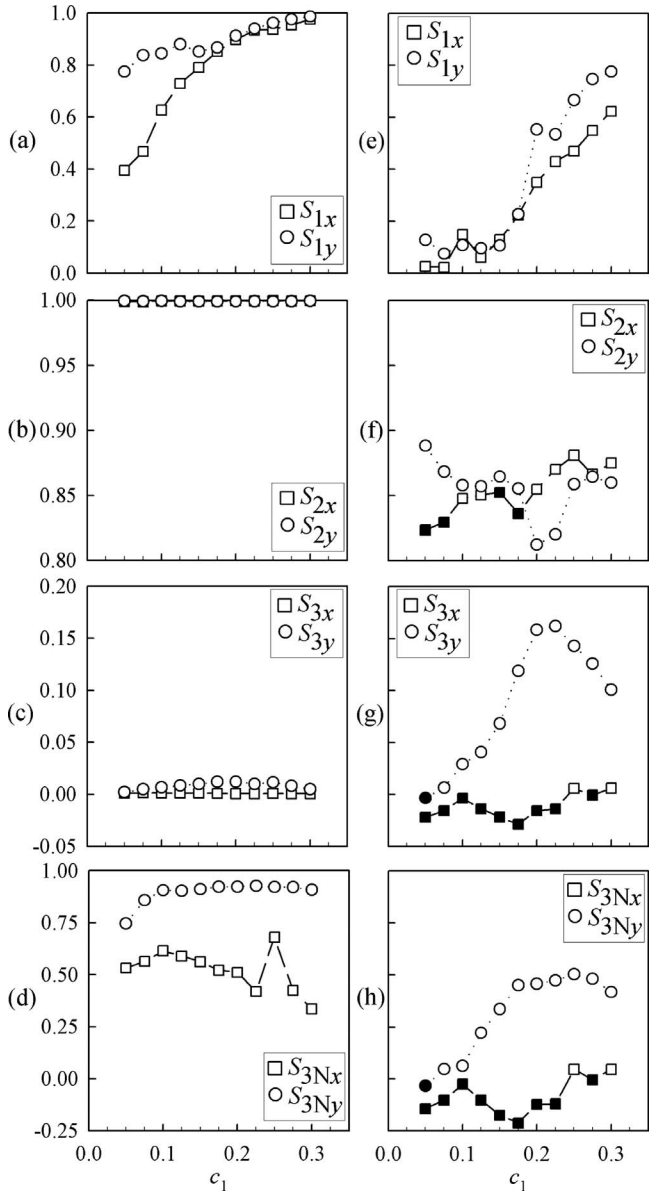

FIG. 5. Same as Fig. 4 for bidirectionally coupled nonidentical Henon maps [Eq. (11), $b=0.1$].

rectional coupling with prevalence in the direction from x to y. The case $c_1=0.3$ for identical systems is particular as it leads to identical synchronization [12], and thus results reproduce those obtained with $c=1$ in Eq. (10).

As with the unidirectional coupling condition, even in bidirectional coupling cross prediction reflects the degree of coupling (S_1 increases with c_1), while mixed prediction (index S_2) and predictability improvement (indices S_3 and S_{3N}) do not exhibit clear trends related to the coupling strength. Cross prediction is also able to detect all coupling conditions, as S_1 is always significant in both identical and nonidentical systems, even in the presence of noise. The same results hold for mixed prediction, even though S_2 seems less robust against noise corruption as in some cases [Figs. 4(f) and 5(f)] either S_{2x} or S_{2y} are insignificant. On the other hand, S_1 and S_2 seem not able to distinguish bidirectional from unidirectional coupling, since their behavior did not substantially change for bidirectionally coupled compared to unidirectionally coupled maps. In addition, no reliable information about coupling direction can be inferred from S_1 and S_2. For instance, in most cases we observe $S_{1y} \geqslant S_{1x}$ [Figs. 4(a), 4(e), 5(a), and 5(e)], which is an opposite result of that found in the previous examples with unidirectional interaction, even though the largest coupling is still set in the direction from x to y. Moreover, asymmetries in coupling of S_1 and S_2 exhibit a behavior dependent on the coupling strength.

The interdependence measures based on predictability improvement result less sensitive to low coupling strengths, as shown, for instance, with $c_1=c_2=0.05$, where both S_{3x} and S_{3y}, as well as S_{3Nx} and S_{3Ny}, are not significant [Figs. 4(c), 4(d), 4(g), 4(h), 5(g), and 5(h)]. Nevertheless, predictability improvement seems suitable to elicit the direction of interaction also in bidirectional coupling, as we observe $S_{3y} \geqslant S_{3x}$ and $S_{3Ny} \geqslant S_{3Nx}$ in all conditions. Another interesting finding is that in nonidentical systems S_3 and S_{3N} are significant for both time series [Figs. 5(c) and 5(d)], thus assessing Granger causality in both directions and distinguishing, in terms of predictability improvement, bidirectional coupling from the unidirectional coupling where only S_{3x} and S_{3Nx} were significant [Figs. 3(c) and 3(d)]. A similar behavior is observed in identical systems [Fig. 4(c)], except for the fact that S_{3x} and S_{3Nx} are sometimes negative. Noise has the effect of masking these results, as the lower coupling from y to x results often negative [Figs. 4(g), 4(h), 5(g), and 5(h)]. Again, utilization of the normalized predictability improvement [indices S_{3Nx} and S_{3Ny}, Figs. 4(d), 4(h), 5(d), and 5(h)] in place of the non-normalized indices (S_{3x} and S_{3y}) leads to similar results due to the fact that the self-predictability of bidirectionally coupled maps is substantially unmodified at varying the coupling strength.

C. Uncoupled systems

In the previous simulations we have addressed the ability of the four coupling measures to characterize the interdependence between coupled systems with different features. However, it is important also to evaluate whether such measures are able to detect correctly the absence of interaction between two dynamical systems. To this end, we eventually consider the case of two uncoupled Henon maps. This situation was reproduced simply by forcing $c=0$ in Eq. (10). Results for the case of uncoupled nonidentical systems without noise contamination are shown as BPMs in Fig. 1(c). The corresponding coupling indices for this example are $S_{1x}=0.031$, $S_{1y}=0.030$ [see the dark colors in the first column of the two BPMs in Fig. 1(c)]; $S_{2x}=0.996$, $S_{2y}=0.999$; $S_{3x}=-0.0041$, $S_{3y}=-0.0001$; and $S_{3Nx}=-20.5$, $S_{3Ny}=-9$.

Uncoupling indices are reported at $c=0$ in Figs. 2 and 3. The case of identical systems without noise is misleading, since setting $b=0.3$ and $c=0$ in Eq. (10) leads to perfectly identical x and y series, which are obviously seen as perfectly coupled rather than uncoupled, so that the indexes with $c=0$ in Figs. 2(a)–2(d) are exactly the same as with $c=1$. The inclusion of noise (specifically the system noise) made the two dynamics fully uncoupled, and this condition was detected by all the three approaches as S_1, S_2, and S_3 (or

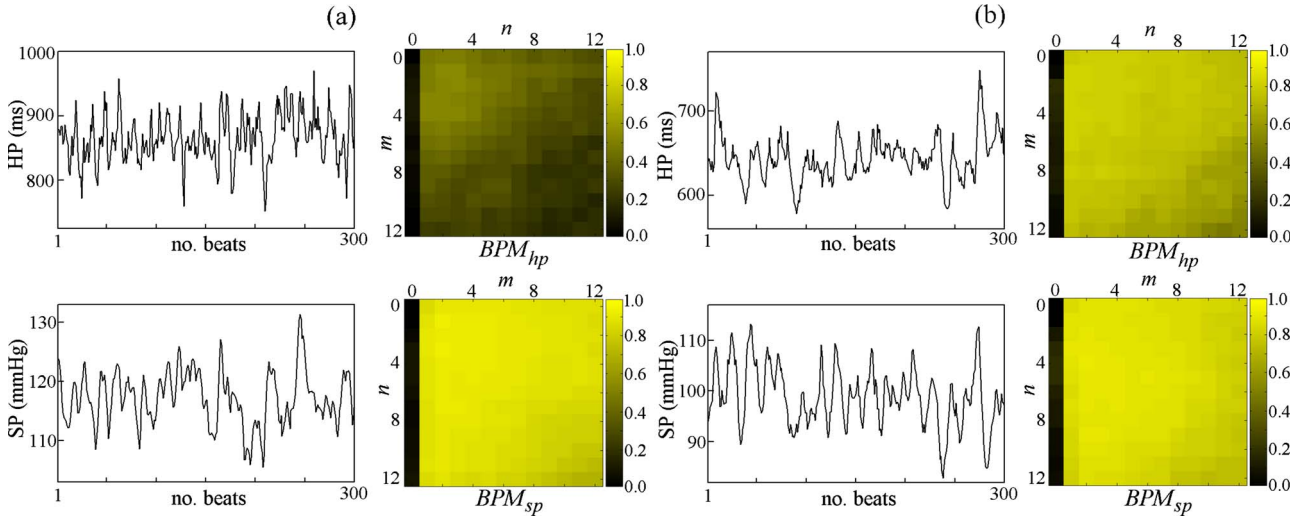

FIG. 6. (Color online) Time series of the heart period (HP) and the systolic pressure (SP) for a typical subject, along with the corresponding bivariate predictability maps (BPM_{hp} and BPM_{sp}, respectively) calculated by mutual nonlinear prediction (a) in the supine position and (b) in the upright position.

S_{3N}) did not exceed the surrogate threshold for significance [Figs. 2(e)–2(h)]. With $b=0.3$ and $c=0$ in Eq. (10) we have nonidentical uncoupled systems generating uncoupled series even in the noise free case [Figs. 3(a)–3(d)]. In this condition S_2, S_3, and S_{3N} are not statistically significant, while S_{1x} and S_{1y} are small, but surprisingly larger than the threshold for significance, suggesting that cross prediction is more inclined to generate false positives in coupling detection. In the noise condition, all measures were below the zero-level threshold [Fig. 3(e)–3(h)].

IV. APPLICATION TO CARDIOVASCULAR DATA

In order to demonstrate the usefulness of mutual nonlinear prediction in a physiological field where commonly only short time series (few hundred samples) are available due to stationarity constraints, we describe the application to the study of the interactions between heart rate and arterial blood pressure measured from humans. These two variables are known to be mutually interacting, as a result of the feedback baroreflex neural regulation, whereby changes in arterial pressure are sensed by the baroreceptors triggering modifications of the heart rate via sympathetic and parasympathetic neural circuits [33], and the feedforward circulatory mechanics, whereby variations of the heart rate induce mechanical variations in the arterial pressure according to Starling law and Windkessel effects [34]. The interdependence between heart rate and arterial pressure variability is studied in healthy subjects during a normal physiological condition (i.e., the resting supine position) and in a condition that is expected to alter the balance between sympathetic and parasympathetic neural regulations (i.e., the upright position after head up tilt) [33]. The two time series under analysis are the heart period (HP) variability, measured as the sequence of the time intervals occurring between consecutive heartbeats, and the systolic pressure (SP) variability, obtained taking the consecutive local maxima of the arterial pressure signal within each detected heart period. We consider 15 young healthy subjects, in whom stationary segments of 300 points are synchronously selected for the HP and SP series in both the supine and upright positions. Details about the study population and the acquisition protocol can be found in Ref. [18]. In all subjects, the analysis is carried out with embedding lag $l=1$ and using $k=30$ neighbors for local linear prediction. The coupling measures of Eqs. (6)–(8) are taken after varying the parameters m and n between 1 and 12.

After normalization, the selected HP and SP variability series are denoted with *hp* and *sp*, respectively. Figure 6 reports an example of the HP and SP series for a typical subject in the supine and upright positions, along with the corresponding BPMs. In the supine position, the predictability measured by the BPM is lower for the HP series (dark colors in BPM_{hp}) than for the SP series [light colors in BPM_{sp}, Fig. 6(a)], while it increases after tilt so that both series are highly predictable in the upright position [Fig. 6(b), lighter colors in the two BPMs]. These behaviors are reproduced also for the self-predictability of the two series (P_S function, first row of each BPM). The maximum cross predictability (i.e., the maximum of the P_C function, first column of each BPM) is statistically significant in the supine position for both series ($S_{1sp}=0.089$, $S_{1hp}=0.105$) and increases in the upright position ($S_{1sp}=0.186$, $S_{1hp}=0.173$). The maximum mixed predictability (i.e., the maximum of the P_M function) is higher for SP ($S_{2sp}=0.923$) than for HP ($S_{2hp}=0.537$) at rest and is high for both series after tilt ($S_{2sp}=0.906$, $S_{2hp}=0.827$). The predictability improvement is statistically significant according to the surrogate data test, with coupling values $S_{3sp}=0.018$, $S_{3hp}=0.039$ at rest and $S_{3sp}=0.018$, $S_{3hp}=0.025$ after tilt. The normalized predictability improvement was higher for the SP series ($S_{3Nsp}=0.192$) than for the HP series ($S_{3Nhp}=0.079$) at rest and was more balanced ($S_{3Nsp}=0.162$, $S_{3Nhp}=0.125$) after tilt.

All these results are common for the considered population and are indeed confirmed by the statistical analysis performed for the 15 subjects. Figure 7 depicts the results ob-

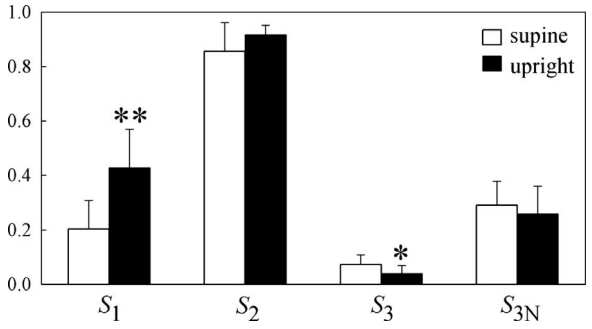

FIG. 7. Nondirectional coupling values between heart period and systolic pressure measured by cross prediction (S_1), mixed prediction (S_2), predictability improvement (S_3), and normalized predictability improvement (S_{3N}) in the supine position (white) and the upright position (black), represented as mean+standard deviation over the 15 considered subjects. The probability that two sets of S values are drawn from the same population, according to the student t-test for paired data: (**) $p<0.001$ and (*) $p<0.01$ supine vs upright.

tained calculating the nondirectional coupling indices on bivariate cardiovascular variability series. All indices indicated the presence of a significant interdependence between HP and SP series in both body positions, as S_1, S_2, S_3, and S_{3N} were always larger than the surrogate threshold for significance in at least one of the two causal directions. The statistically significant increase of the index S_1 moving from the supine to the upright position seen in Fig. 7 is well interpretable on the basis of the known cardiovascular physiology. Indeed, it reflects the increased strength of interaction between the two cardiovascular variables after head-up tilt, as an effect of the activation of the sympathetic nervous system that enhances primarily the feedback baroreflex regulation from SP to HP and, consequently, the feedforward influence of HP on SP [18,33]. On the contrary, the interpretation of other nondirectional coupling indices is less intuitive. Mixed prediction yields a larger predictability than cross prediction (S_2 is higher than S_1 in Fig. 7), as a consequence of the quote of self-predictability captured by using mixed states. This aspect has also the detrimental effect of masking modifications of the corresponding interdependence measure with varying physiological conditions: the increase of S_2 moving from the supine to the upright position is indeed blunted and is not statistically significant. Even the interpretation of the significant decrease of the predictability improvement from rest to tilt may be misleading, since the absolute values of the index S_3 are directly influenced by the self-predictability of the time series under analysis [see Eq. (6)]. In this case, the self-predictability of the cardiovascular series improves significantly with the tilt transition, as we obtained $\max_m\{P_{Ssp}(m)\}=0.81$ at rest and $\max_m\{P_{Ssp}(m)\}=0.87$ after tilt for the SP and $\max_n\{P_{Shp}(n)\}=0.59$ at rest and $\max_n\{P_{Shp}(n)\}=0.85$ after tilt for the HP. After normalization (index S_{3N}), no significant modifications of the predictability improvement are indeed observed. These observations confirm on experimental data that cross prediction is more suitable than mixed prediction and predictability improvement for quantifying the degree of the interaction in bivariate time series and substantiate the formulation of previously proposed approaches estimating the coupling strength without considering past self-influences of the analyzed time series [3,28].

Results of the directional coupling analysis applied to SP and HP variability are summarized in Fig. 8. Cross prediction confirms for both series the increase of coupling consequent to tilt, while S_{1sp} and S_{1hp} were substantially balanced in both body positions [Fig. 8(a)]. Mixed prediction indicates an unbalancing in the coupling in supine subjects [Fig. 8(b)]. However, we suggest a very cautious interpretation of these results, since simulations have shown that cross and mixed predictions can hardly elicit the direction of coupling in short bivariate time series. The predictability improvement was always significant, as S_{3sp} and S_{3hp} were positive and larger than the surrogate threshold for significance (except for S_{3hp} in one subject at rest and S_{3sp} in one subject after tilt). This result indicates the bidirectional nature of the interaction between HP and SP in both body positions, in accordance with the expected physiological behavior [33,34]. The values of S_{3sp} and S_{3hp} indicate a tendency to decrease of the predictability improvement from the supine to the upright position [Fig. 8(c)]. However, as above discussed, in this application the index is biased by the variable self-predictability of the investigated time series. Utilization of the normalized predictability improvement, which prevents the predictability of the single time series from affecting the directionality measure, reveals very interesting results [Fig. 8(d)]. First, we observe a higher predictability improvement from HP to SP (index S_{3Nsp}) than in the opposite direction (index S_{3Nhp}) in the supine position. This result supports, from the different point of view provided by mutual nonlinear prediction, the notion that nonbaroreflex or nonautonomic mechanisms operating in the direction from HP to SP through the circulatory mechanics [35] play a major role in the cardiovascular regulation of supine humans [18,36]. Nevertheless, the assumption of the upright position seems to produce an enhancement of the interactions along the baroreflex pathway from SP to HP, as documented by the significant increase of S_{3Nhp} moving from rest to tilt conditions. This increase, leading to a balanced SP-HP regulation in the upright position, is compatible with the activation of the sympathetic branch of the autonomic nervous system induced by tilt [33].

V. CONCLUSIONS

In this work we compared both on simulations and on real data the performance of different previously proposed mutual nonlinear prediction approaches [9,11,12] with regard to their ability to evaluate coupling strength and causality in bivariate time series measured from coupled systems. Our results support the feasibility of mutual nonlinear prediction for detecting different coupling conditions even in short (few hundred samples) realizations of the observed dynamics, but suggest that different prediction schemes have different abilities in detecting coupling strength and directionality of the interactions.

We found that mutual nonlinear prediction performed through cross prediction [9] is suitable to detect the interaction between short coupled series and to quantify its strength,

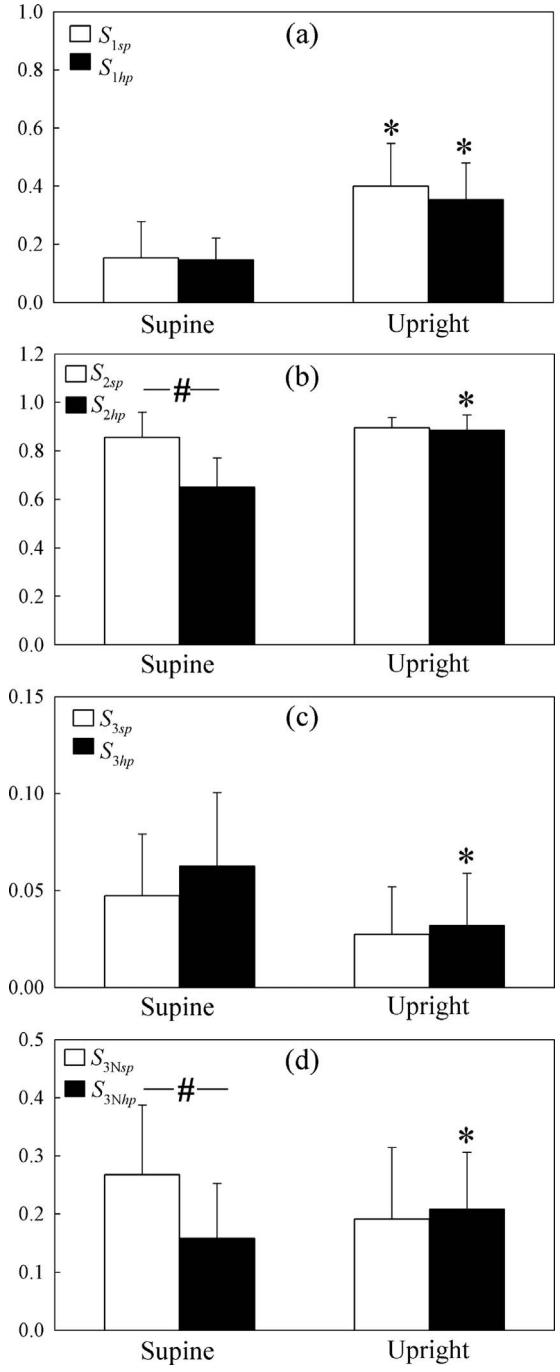

FIG. 8. Directional coupling values measured by cross prediction [(a) S_1], mixed prediction [(b) S_2] predictability improvement [(c) S_3], and normalized predictability improvement [(d) S_{3N}] for the systolic pressure (*sp*, white) and the heart period (*hp*, black) variability series in the supine and the upright positions, represented as mean+standard deviation over the 15 considered subjects. The probability that two sets of S values are drawn from the same population, according to the student t-test for paired data: (*) $p<0.05$ supine vs upright and (#) $p<0.05$ S_{sp} vs S_{hp}.

as the corresponding interdependence measure was related to the coupling degree imposed in both unidirectionally and bidirectionally coupled Henon maps and reflected the expected coupling increase moving from the supine to the upright position in the study of heart-rate–arterial-pressure interactions. However, cross prediction seems unable to distinguish unidirectional from bidirectional simulated interactions. Moreover, it turns out to be unreliable to infer the direction of coupling from the asymmetrical values of the coupling measure, as our simulations clearly show that the observed asymmetries were not stable at varying the dynamical properties of the systems, the imposed coupling degree, and the noise conditions. This observation agrees with previous studies arguing that it is very difficult to obtain nontrivial directional information from asymmetries observed from nonlinear interdependence measures based on quantifying state space correspondences in coupled systems [17,20].

The approach based on mixed prediction [11] provided behaviors that resemble those of cross prediction, with the drawback that results were more difficult to interpret as a consequence of the presence of a quote of self-predictability affecting the value of the coupling measure. This aspect, which is a direct consequence of the utilization of mixed patterns including points of both series for performing mutual prediction, led to the presence of high coupling values even for weakly coupled signals and, in the real data application, to a more problematic detection of known physiological behaviors, such as the increase of heart-rate–arterial-pressure coupling expected with the transition from supine to upright. Nevertheless, mixed prediction used together with the proposed surrogate data approach was able to reveal the absence of coupling in all the simulations where independent signals were generated.

When interdependence was assessed evaluating the improvement in predictability given by mixed prediction with respect to self-prediction [12], simulations evidenced a weaker capability to detect conditions of low coupling. Moreover, the index did not reflect the actual coupling strength, as it tends to decrease when the interacting systems approached the synchronized state. Nevertheless, the index resulted as the most appropriate to distinguish unidirectional from bidirectional coupling and to infer the direction of coupling based on asymmetries emerging from its calculation along the two causal directions. Indeed, simulations showed that a larger predictability improvement was always noticed in the causal direction on which the higher coupling was imposed, and the reported asymmetry was preserved at varying the coupling strength and was even enhanced in presence of noise. Finally, we observe that in practical applications where different conditions are compared, measures of predictability improvement normalized to the unpredictability of the observed time series [14] should be used. This correction allows us to release the coupling measure from accounting for the intrinsic predictability of the single time series, which can be different for the two considered series and can vary with the experimental conditions. Using normalized predictability improvements for the causal analysis of cardiovascular interactions in healthy humans, we showed indeed (i) an asymmetrical relationship in the resting supine position that was related to the prevalence of the mechanical effects of heart rate on arterial pressure over the neural modulation from arterial pressure to heart rate and (ii) an increase in the directional influence of arterial pressure on heart rate after head-up tilt, which was ascribed to the intensified stimulus on the baroreceptors in the upright position.

[1] E. Pereda, R. Q. Quiroga, and J. Bhattacharya, Prog. Neurobiol. **77**, 1 (2005).
[2] X. Xiao, T. J. Mullen, and R. Mukkamala, Physiol. Meas **26**, R41 (2005); E. Pereda, D. M. de La Cruz, L. De Vera, and J. J. Gonzalez, IEEE Trans. Biomed. Eng. **52**, 578 (2005); A. Porta *et al.*, Med. Biol. Eng. Comput. **38**, 180 (2000); J. P. Saul *et al.*, Am. J. Physiol. **261**, H1231 (1991).
[3] G. Nollo *et al.*, Am. J. Physiol. Heart Circ. Physiol. **283**, H1200 (2002).
[4] A. Kraskov, H. Stogbauer, and P. Grassberger, Phys. Rev. E **69**, 066138 (2004); T. Schreiber, Phys. Rev. Lett. **85**, 461 (2000); M. Palus, V. Komàrek, Z. Hrncìr, and K. Sterbovà, Phys. Rev. E **63**, 046211 (2001).
[5] M. G. Rosenblum, A. S. Pikovsky, and J. Kurths, Phys. Rev. Lett. **76**, 1804 (1996); C. Schafer, M. G. Rosenblum, J. Kurths, and H. H. Abel, Nature (London) **392**, 239 (1998); A. Pikovsky, M. G. Rosenblum, and J. Kurths, *Synchronization—A Universal Concept in Nonlinear Sciences* (Cambridge University Press, Cambridge, England, 2001).
[6] N. F. Rulkov, M. M. Sushchik, L. S. Tsimring, and H. D. I. Abarbanel, Phys. Rev. E **51**, 980 (1995).
[7] J. Arnhold, P. Grassberger, K. Lehnertz, and C. E. Elger, Physica D **134**, 419 (1999).
[8] R. Quian Quiroga, A. Kraskov, T. Kreuz, and P. Grassberger, Phys. Rev. E **65**, 041903 (2002).
[9] S. J. Schiff, P. So, T. Chang, R. E. Burke, and T. Sauer, Phys. Rev. E **54**, 6708 (1996).
[10] M. Le Van Quyen, J. Martinerie, C. Adam, and F. J. Varela, Physica D **127**, 250 (1999); M. Le Van Quyen *et al.*, Brain Res. **792**, 24 (1998).
[11] M. Wiesenfeldt, U. Parlitz, and W. Lauterborn, Int. J. Bifurcation Chaos Appl. Sci. Eng. **11**, 2217 (2001).
[12] U. Feldmann and J. Bhattacharya, Int. J. Bifurcation Chaos Appl. Sci. Eng. **14**, 505 (2004).
[13] N. Ancona, D. Marinazzo, and S. Stramaglia, Phys. Rev. E **70**, 056221 (2004).
[14] D. Marinazzo, M. Pellicoro, and S. Stramaglia, Phys. Rev. E **73**, 066216 (2006); Y. Chen, G. Rangarajan, J. Feng, and M. Ding, Phys. Lett. A **324**, 26 (2004).
[15] L. Faes and G. Nollo, Med. Biol. Eng. Comput. **44**, 383 (2006); L. Faes, R. Cucino, and G. Nollo, Biomed. Tech. **51**, 255 (2006); L. Faes, A. Porta, and G. Nollo (unpublished).
[16] C. W. J. Granger, J. Econ. Dyn. Control **2**, 329 (1980); K. Hlavàckovà-Schindler, M. Palus, M. Vejmelka, and J. Bhattacharya, Phys. Rep. **441**, 1 (2007).
[17] R. Quian Quiroga, J. Arnhold, and P. Grassberger, Phys. Rev. E **61**, 5142 (2000).
[18] G. Nollo *et al.*, Am. J. Physiol. Heart Circ. Physiol. **288**, H1777 (2005).
[19] M. G. Rosenblum and A. S. Pikovsky, Phys. Rev. E **64**, 045202(R) (2001); M. G. Rosenblum, L. Cimponeriu, A. Bezerianos, A. Patzak, and R. Mrowka, *ibid.* **65**, 041909 (2002); M. Palus and M. Vejmelka, *ibid.* **75**, 056211 (2007); A. Porta *et al.*, Biol. Cybern. **86**, 241 (2002).
[20] A. Schmitz, Phys. Rev. E **62**, 7508 (2000).
[21] N. Wiener, in *Modern Mathematics for Engineers*, edited by E. F. Beckenbach (McGraw-Hill, New York, 1956).
[22] C. W. J. Granger, Econometrica **37**, 424 (1969).
[23] J. D. Farmer and J. J. Sidorowich, Phys. Rev. Lett. **59**, 845 (1987).
[24] M. Casdagli, Physica D **35**, 335 (1989).
[25] A. Porta *et al.*, IEEE Trans. Biomed. Eng. **54**, 94 (2007).
[26] F. Takens, in *Dynamical Systems and Turbulence*, edited by D. Rand and S. L. Young (Springer-Verlag, Berlin, 1981), Vol. 898.
[27] J. Theiler, Phys. Rev. A **34**, 2427 (1986).
[28] A. Porta *et al.*, Biol. Cybern. **81**, 119 (1999).
[29] T. Schreiber and A. Schmitz, Physica D **142**, 346 (2000).
[30] J. Theiler *et al.*, Physica D **58**, 77 (1992); M. Palus and D. Hoyer, IEEE Eng. Med. Biol. Mag. **17**, 40 (1998); D. Prichard and J. Theiler, Phys. Rev. Lett. **73**, 951 (1994).
[31] J. Bhattacharya, E. Pereda, and H. Petsche, IEEE Trans. Syst. Man Cybern., Part A. Syst. Humans **33**, 85 (2003).
[32] R. G. Andrzejak, A. Kraskov, H. Stogbauer, F. Mormann, and T. Kreuz, Phys. Rev. E **68**, 066202 (2003).
[33] A. Malliani, *Principles of Cardiovascular Neural Regulation in Health and Disease* (Kluwer, Norwell, MA, 2000).
[34] H. P. Koepchen, in *Mechanisms of Blood Pressure Waves* (Springer, Berlin, 1984).
[35] T. J. Mullen *et al.*, Am. J. Physiol. **272**, H448 (1997).
[36] S. C. Malpas, Am. J. Physiol. Heart Circ. Physiol. **282**, H6 (2002).